Research Article
Analysis of a T-Frame Bridge

Pengzhen Lu,[1, 2, 3] Fangyuan Li,[4] and Changyu Shao[2]

[1] Faculty of Civil Engineering and Architecture, Zhejiang University of Technology,
   Hangzhou 310014, China
[2] Shanghai Municipal Engineering Design and Research Institute, Shanghai 200092, China
[3] Department of Civil Engineering, Zhejiang University, Hangzhou 310027, China
[4] College of Civil Engineering, Tongji University, Shanghai 200092, China

Correspondence should be addressed to Fangyuan Li, fyli@tongji.edu.cn

The structural behavior of T-frame bridges is particularly complicated and it is difficult using a general analytical method to directly acquire the internal forces in the structure. This paper presents a spatial grillage model for analysis of such bridges. The proposed model is validated by comparison with results obtained from field testing. It is shown that analysis of T-frame bridges may be conveniently performed using the spatial grillage model.

1. Introduction

Rigid frame bridges are appearing in various exotic forms resulting in complex, efficient, and aesthetically pleasing structures, with graceful appearance, compact construction dimension, spacious room under bridge, and a broad eye view, and the plan can be applied to the construction of long span bridges. Because of T-frame bridge special advantages in the rigid frame bridge, more and more the T-frame bridges were used. The safety of the T-frame bridges presents an increasing important concern in design, construction, and service. This special type of flexible, large span T-frame bridges makes the structural analysis more complex and difficult [1–3].

Typically, the design of highway bridges in China must conform to the General Code for Design of Highway Bridges and Culverts (JTG D60-2004) specifications. The analysis and design of any highway bridge must consider truck and lane loadings. However, the structural behavior of T-frame bridge is particularly complicated, and many rigorous methods for analysis of T-frame bridges are quite tedious and often difficult.

Pan et al. [1] carried out uncertainty analysis of creep and shrinkage effects in long-span continuous rigid frame of Sutong Bridge. Azizi et al. [4] used spectral element method for analyzing continuous beams and bridges subjected to a moving load. Wang et al. [5] analyzed dynamic behavior of slant-legged rigid-frame Highway Bridge. Dicleli [6] presented a computer-aided approach of integral-abutment bridges, and an analysis procedure and a simplified structure model were proposed for the design of integral-abutment bridges considering their actual behavior and load distribution among their various components [7, 8]. There were several approximate analysis methods for bridge decks, which include the grillage method and the orthotropic plate theory [9]. Yoshikawa et al. [10] investigated construction of Benten Viaduct, rigid-frame bridge with seismic isolators at the foot of piers. Kalantari and Amjadian [11] reported a 3DOFs analytical model an approximate hand method was presented for dynamic analysis of continuous rigid deck.

Mabsout et al. [12] reported the results of parametric investigation using the finite-element analysis of straight, single-span, simply supported reinforced concrete slab bridges. The study considered various span lengths and slab widths, number of lanes, and live loading conditions for bridges with and without shoulders. Longitudinal bending moments and deflections in the slab were evaluated and compared with procedures recommended by AASHTO [13].

In a word, the above mentioned methods can not exactly deal with the structural mechanical behavior of the T-frame bridges what's worse, they may lead to insecurity of structural design. Grillage analysis is probably the most popular computer-aided method for analyzing bridge decks [14, 15]. This is because it is easy to comprehend and use, relatively inexpensive, and it has been proven to be reliably accurate for a wide variety of bridge types [16–19]. The method, pioneered for computer use by Lightfoot and Sawko [20] represented the deck by an equivalent grillage of beams. Based on the grillage method, Hambly [21] produced design charts for the analysis and design of bridge decks. Based on the structure characteristic and the grillage method, analysis of a T-frame bridge based on the grillage method will be represented.

This paper presents a spatial grillage model for the analysis of a T-frame bridge. Static and dynamic analysis results of spatial grillage model for the T-frame bridge are compared with results based on results obtained from field testing. The research results shown that analysis of T-frame bridges may be conveniently performed using the spatial grillage model.

2. Box-Girder Deck Analysis with Spatial Grillage Model

Spatial grillage model is a convenient method for analysis of box-girder bridges. In the model, the box-girder slab is represented by an equivalent grid of beams whose longitudinal and transverse stiffnesses are approximately the same as the local plate stiffnesses of the box-girder slab.

In the spatial grillage model analysis, the orientation of the longitudinal members should be always parallel to the free edges while the orientation of transverse members can be either parallel to the supports or orthogonal to the longitudinal beams. According to the grillage model, the output internal force resultants can be used directly. The grillage model involves a plane grillage of discrete interconnected beams. The representation of a bridge as a grillage is ideally suited for carrying out the necessary calculations associated with analysis and design on a digital computer and it gives the designer an idea about the structural behavior of the bridge.

The main challenge in the spatial grillage model is how to obtain an equivalent grillage based on the box-girder deck structure. The spatial grillage model for analyzing box-girder Slab bridge includes figuring out the grillage mesh and grillage member section properties.

2.1. Spatial Grillage Mesh

Determination of a suitable grillage mesh for a box-girder of rigid frame bridge is, as for a slab deck, best approached from a consideration of the structural behavior of the particular deck rather than from the application of a set of rules. Since the average longitudinal and transverse bending stiffness are comparable, the distribution of load is somewhat similar to that of a torsionally flexible slab, but with forces locally concentrated. The grillage simulates the prototype closely by having its members coincident with the centre lines of the prototypes beams. In addition, there is a diaphragm in the prototype such as over a support, and then a grillage member should be coincident. Based on section shape of the rigid frame bridge and support arrangements, a spatial grillage mesh should be represented by the above mentioned spatial grillage method. At the same time, according to the grillage equivalent theory, the following three important aspects have to be noted: according to mechanical behavior of a rigid frame bridge, one should place the grillage beams along the lines of designed strength; the longitudinal and transverse member spacing should be reasonably similar to permit sensible static distribution of loads; in addition, virtual longitudinal and transverse members are often employed for the sake of convenience in the analysis. The virtual members only offer stiffness, but its weight must be ignored.

2.2. Grillage Member Section Properties

Grillage member section properties include longitudinal grillage member section properties and transverse grillage member section properties. Based on rigid frame bridge structural features, the amount of each deck for prototype bridge is represented by the appropriate grillage member. The flexural inertia of each grillage member is calculated about the centroid of the section it represents. The section properties of a transverse grillage member, which solely represents slab, are calculated as for slab. For this

$$I = \frac{bd^3}{12},$$
$$c = \frac{bd^3}{6}.$$

(2.1)

When the grillage member also includes a diaphragm, an estimate must be made of the width of slab acting as flange. If the diaphragms are at close centres, the flanges of each can be assumed to extend to midway between diaphragms. It is usually conservative to assume that the effective flange is 0.3 of the distance between longitudinal members. The parameters of the grillage member section properties for box-girder are given by

Figure 1: A photo of Quhai T-frame bridge.

$$GJ_x = \frac{E}{2(1+m)},$$

$$GJ_y = \frac{E}{2(1+m)},$$

$$(2.2)$$

where E is the modulus of elasticity, I_x, I_y the moments of inertia, J_x, J_x the moments of torsional inertia, and m the moment per unit width.

3. Illustrative Example

The Quhai rigid frame bridge is over the Qu river in Dongguang, Guangdong province, China. A photo of the bridge just before its opening is shown in Figure 1. The bridge has a single box with double chamber deck construction consisting of 29 spans with an overall length of 768.6 m (19.3 m + 12 × 20 m + 70 m + 110 m + 70 m + 12 × 20 m + 19.3 m). The bridge was completed in 1995. The two-way roadway of the bridge deck is 32 m wide with six lanes. Figure 2 shows the general view of the Quhai rigid frame bridge with schematic plan, elevation, and typical cross section of the single box with double chamber deck.

The Quhai Bridge is a rigid frame design for a single box with double chamber bridge, with two main palaces with hang holes, T-frame of 2 × 40 m, and two hung-girder spans is 30 m. Cantilever root height of box-girder for T-frame is 6 m, and end height is 2 m. A single box with double chamber and 32 m wide section was selected for the bridge superstructure. The design live load of the original bridge is vehicle load, and checking load is trailer-100 (loads specified in the Bridge Design Code of China). In order to increase the bearing capacity of the bridge, new loads specified (truck-20 and trailer-120) were employed for the bridge application.

3.1. Three-Dimensional Finite Element Modeling

Three-dimensional linear elastic finite element models of the spatial grillage model of the Quhai Bridge have been constructed using SAP2000 finite element analysis software. In the finite-element model, 3D beam4 elements were adopted to create the grillage model that will be used to determine the internal stress resultants, natural frequencies, and corresponding mode shapes. The spatial grillage model was shown in Figure 3, and the virtual beams only
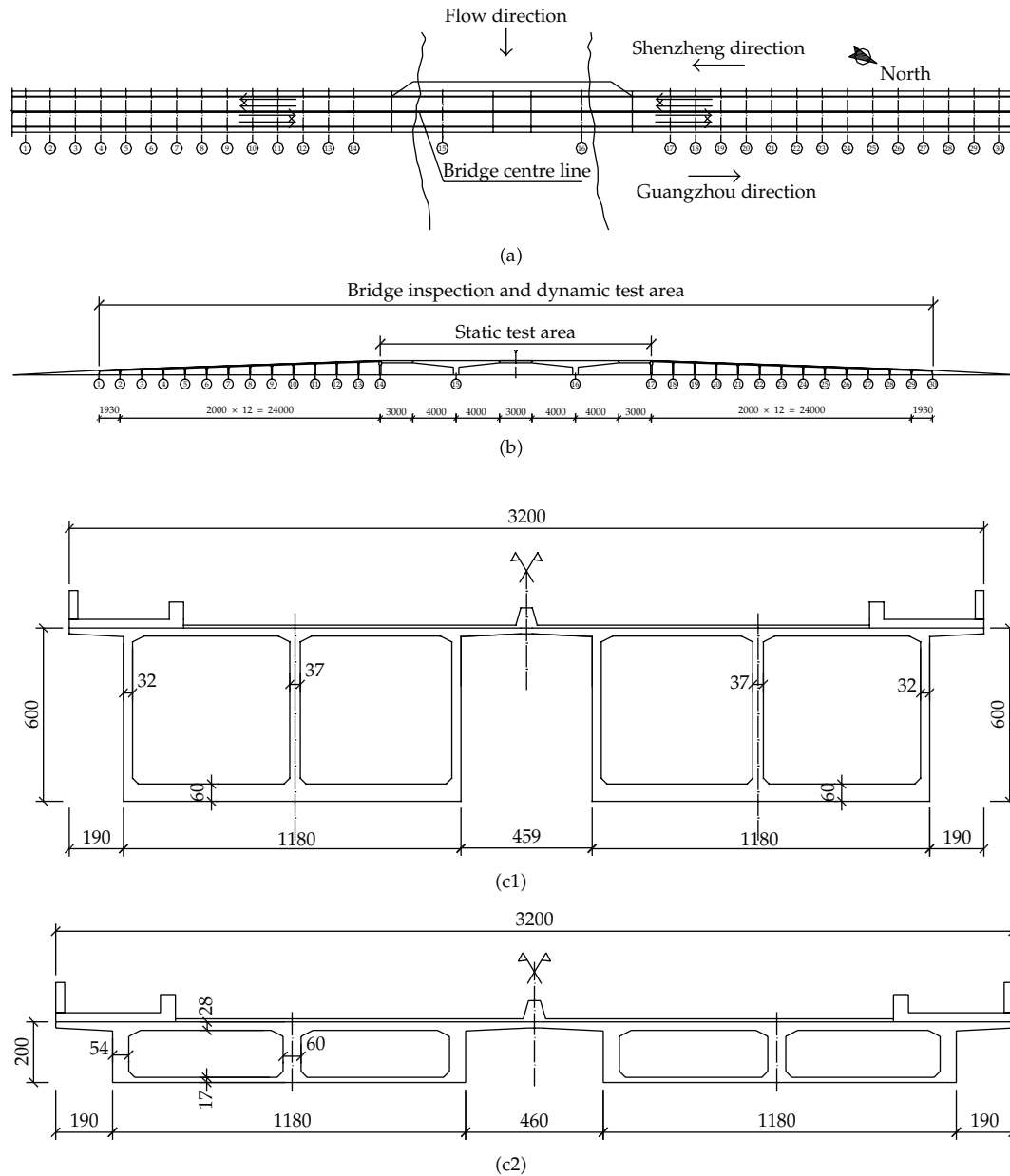
Flow direction

Shenzheng direction

North

Bridge centre line

Guangzhou direction

(a)

Bridge inspection and dynamic test area

Static test area

1930 2000 × 12 = 24000 3000 4000 4000 3000 4000 4000 3000 2000 × 12 = 24000 1930

(b)

3200

32 37 37 32

600 600

60 60

190 1180 459 1180 190

(c1)

3200

28

200 54 60

17

190 1180 460 1180 190

(c2)

Figure 2: General view of Quhai T-frame bridge: (a) plan view; (b) elevation view; (c) typical cross-section of box-girder deck.

offer stiffness. In the finite-element model of the bridge, 3D 1104 elements (beam 4) and 817 nodes were used. The spatial grillage model of the bridge as a whole is shown in Figure 4.

3.2. Results of Static Analysis

According to the influence line method of the control section, internal forces of longitudinal and transverse grillage members were presented. Internal force values of the control section
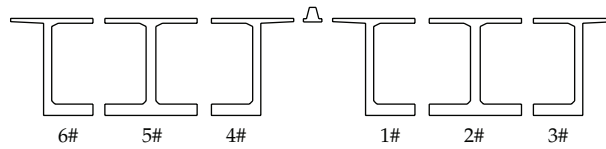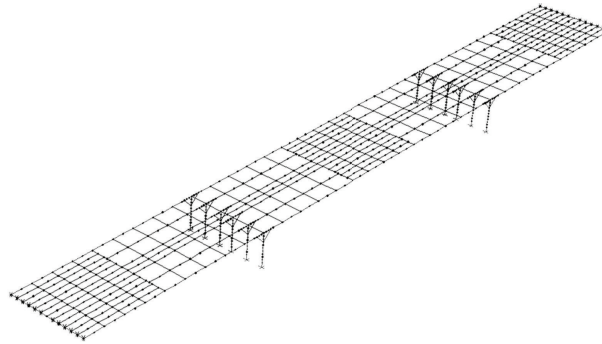
Figure 3: Equivalent grillage model.

Figure 4: Grillage model of main bridge for Quhai Bridge.

for the grillage model were shown in Tables 1 and 2. In accordance with the analytical results of the longitudinal grillage, under trailer-120 load, the maximum normal moment of edge hang beam (1#) was obtained by the mid-span section of the grillage, and the maximum value is 2.0×10^6 N · m; the maximum normal moment of middle hang beam (1#) was obtained by the mid-span section of the grillage, and the maximum value is 2.13×10^6 N · m; under truck 20 and crowd load, the maximum negative moment was proposed by the abutments (15#) section of the grillage, and the maximum value is 2.06×10^7 N · m. In terms of the internal stress resultants, the moment and shear force envelope diagrams of the control grillage model were obtained and shown in Figures 5, 6, and 7.

3.3. Results of Dynamic Analysis

From the dynamic analysis using the spatial grillage model, the first natural frequency of the hang beam (14-15#) and T-frame is 3.6 Hz and 1.31 Hz, respectively, and vibration mode is symmetric vertical bending; the first natural frequency of the hang beam (16-17#) and T-frame is 3.6 Hz and 1.31 Hz, respectively, and vibration mode is symmetric vertical bending; the first natural frequency of the middle-span hang beam is 3.6 Hz, and vibration mode is symmetric vertical bending. The first mode shapes of the bridge are shown in Figure 8.

4. Description of Field Load Tests and Results

The field static or dynamic tests on bridges have been of great interest not only in investigating bridge fundamental behavior but also for calibrating finite-element models. Several results of field tests and correlated finite-element analyses have been presented for the Quhai Bridge. The field load tests on the Quhai Bridge employed the corresponding design load, to simulate the design live loads of the bridge. The field load tests on the Quhai Bridge
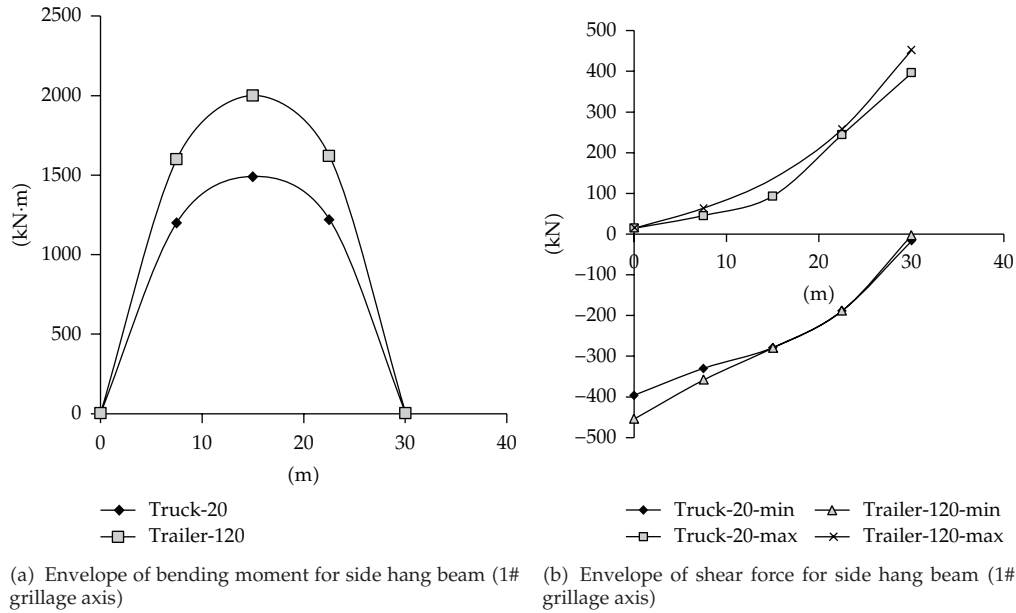
(a) Envelope of bending moment for side hang beam (1# grillage axis)

(b) Envelope of shear force for side hang beam (1# grillage axis)

Figure 5: Envelope of internal force of grillage model for side hang beam (1# grillage).

Table 1: Moment under design live load (control sections of 1# grillage/N·m).

Section location	Trailer 120 max/min	Truck 20 max/min	Control moment
Pier (14#)	0/0	0/0	0/0
0.5 L	$3.9E+6/-2.4E+4$	$2.9E+6/-3.1E+5$	$3.9E+6/-3.1E+5$
Corbel	0/0	0/0	0/0
Pier (15#)	$0/-3.5E+7$	$0/-4.1E+7$	$0/-4.1E+7$
Corbel	$0/-5.6E+3$	$0/-1.1E+4$	$0/-1.1E+4$
0.5 L	$4.2E+6/-2.4E+4$	$3.2E+6/-3.3E+5$	$4.3E+6/-3.3E+5$
Corbel	0/0	0/0	0/0
Pier (16#)	$0/-3.5E+7$	$0/-4.1E+7$	$0/-4.1E+7$

Table 2: Shear force under design live load (control sections of 1# grillage/N).

Section location	Trailer 120 max/min	Truck 20 max/min	Control moment
Pier (14#)	$5.3E+2/-9.1E+5$	$2.9E+4/-7.9E+5$	$9.1E+5$
0.5 L	$2.7E+5/-5.7E+5$	$1.8E+5/-5.5E+5$	$5.7E+5$
Corbel	$9.1E+5/-6.1E+3$	$7.9E+5/-3.3E+4$	$9.1E+5$
Corbel	$8.6E+5/0$	$7.4E+5/0$	$8.6E+5$
Pier (15#)	$1.1E+6/0$	$1.7E+6/0$	$1.7E+6$
Pier (15#)	$0/-1.1E+6$	$0/-1.7E+6$	$1.7E+6$
Corbel	$0/-8.6E+5$	$0/-7.5E+5$	$8.6E+5$
Corbel	$6.2E+3/-9.7E+5$	$3.8E+4/-8.8E+5$	$9.7E+5$
0.5 L	$3.1E+5/-5.5E+5$	$2.1E+5/-5.5E+5$	$5.5E+5$
Corbel	$9.1E+5/-6.1E+3$	$7.9E+5/-3.5E+4$	$9.1E+5$
Corbel	$8.6E+5/0$	$7.5E+5/0$	$8.6E+5$
Pier (16#)	$1.1E+6/0$	$1.7E+6/0$	$1.7E+6$
Pier (16#)	$0/-1.1E+6$	$0/-1.7E+6$	$1.7E+6$

(a) Envelope of bending moment for T-frame (1# grillage axis)

(b) Envelope of shear force for T-frame (1# grillage axis)
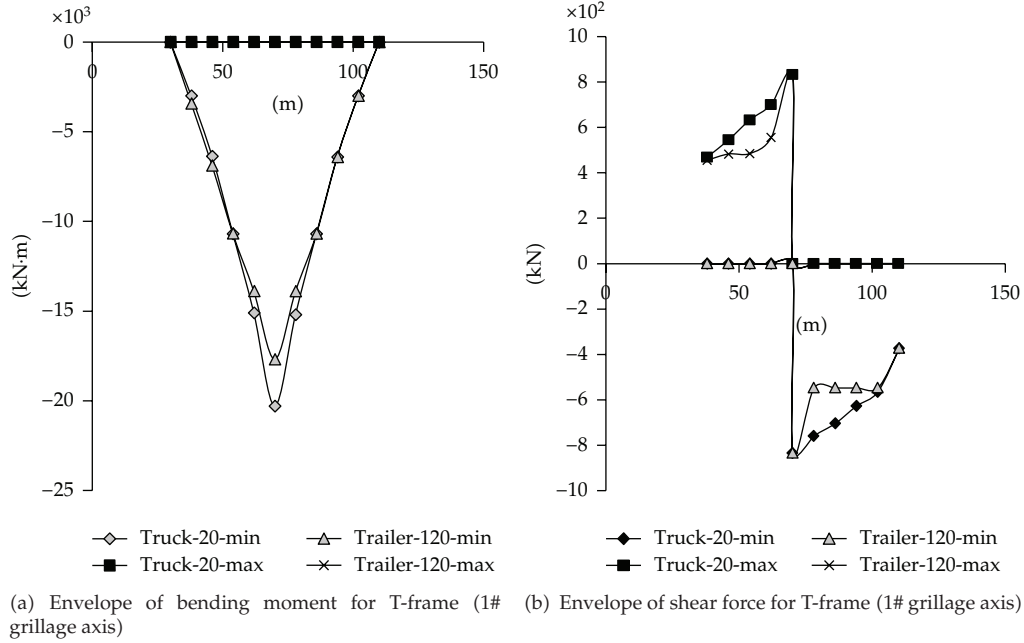
Figure 6: Envelope of internal force of grillage model for T-frame (1# grillage).

(a) Envelope of bending moment for middle hang beam (1# grillage axis)

(b) Envelope of shear force for middle hang beam (1# grillage axis)
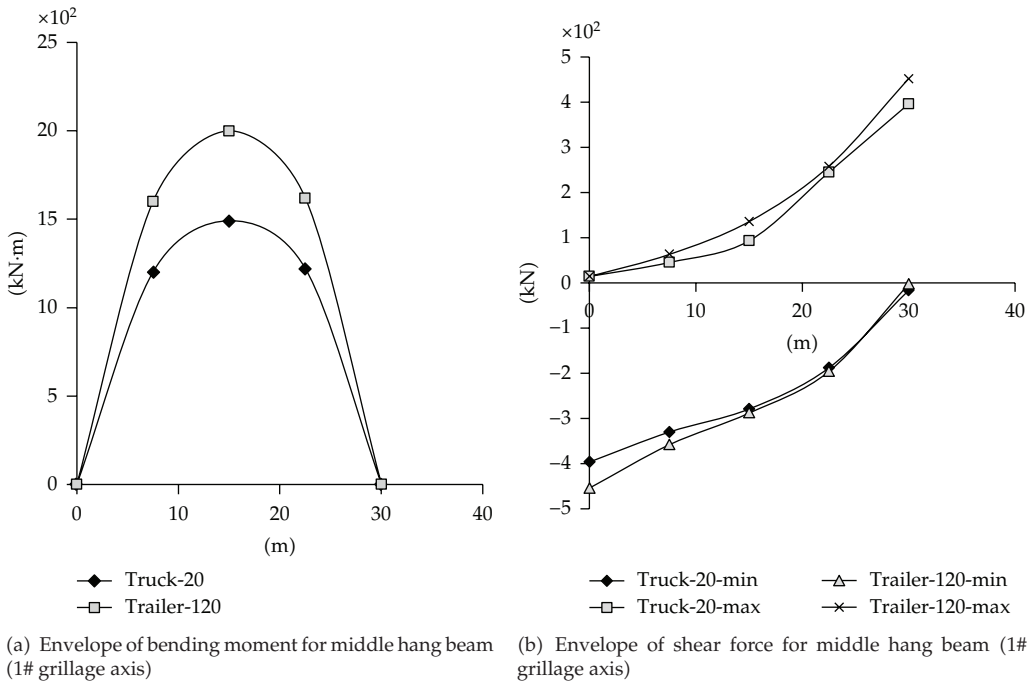
Figure 7: Envelope of internal force of grillage model for middle hang beam (1# grillage).

(a) The first vibration mode of T-frame

(b) The first vibration mode of hang beam (14-15# and 16-17#)

(c) The first vibration mode of hang beam (15-16#)
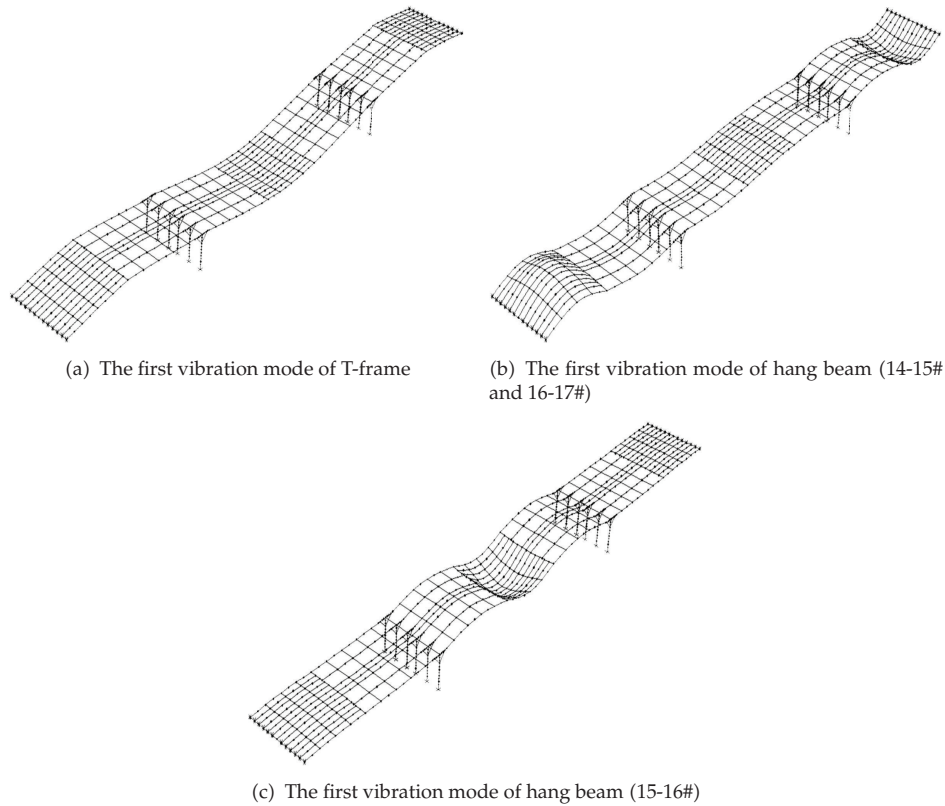
Figure 8: the first vibration mode of grillage model for hang beam and T-frame.

employed the heavily loaded dump trucks, each with approximately 30t weight, to simulate the design live loads of the bridge. Due to the difficulty to hire the same type of such heavy dump trucks in the area, there were, in total, 5 trucks employed during the static load tests. The individual axle load and spacing of each dump truck were carefully measured at the nearby weight station before it was moved to the bridge.

In addition, the applied test loads should be identical to the design live loads of the bridge. The applied test loads are normally designated by the static test load efficiency:

$$\eta = \frac{S_t}{S_d(1 + \mu)},$$

(4.1)

where S_t is the resultant force at the specified section under the planned static test loads; S_d is the resultant force at the same specified section under the design live loads; μ is the impact factor used in the design of the bridge. All test load efficiency η values are within 0.8–1.05, which demonstrates the validity of the statically loaded tests on the bridge. As a result, a total of 27 measuring points of the deflection were set, and 54 strained measuring points were measured. The test setup included strained measurements and deflection measurements at control section. The three load cases during the field tests are shown in Figure 9.

(a)

(b)

(c)

Figure 9: Photos of three critical load cases: (a) field loading on the main span (16-17#); (b) field loading on the main span (14-15#); (c) field loading on the main span (15-16#).

4.1. Results of Deflection Test

Deflection values of the prototype bridge for the corresponding grillage under working condition I and working condition II are shown in Figure 10, and deflection values of the prototype bridge for the corresponding grillage under working condition III are shown in Figure 11. Measure point (5#) is a control point in the regions of the largest deformation cross-section and its corresponding maximum value is −23.6 mm. The maximum theoretic deformation of the measure point for control section is −26.3 mm, and the ratio α between the experimental and theoretical value is 0.9, and it is within the range of the national standard ($0.7 \leq \alpha \leq 1.05$). Maximum values of control section deflection of the field test are also in the range of national standard ($[f] \leq l/600 = 116.67$ mm). The results of measured deflection show that all values of measured deflections satisfied the design requirements. This indicates that the bridge possesses the adequate strength to resist the loadings.
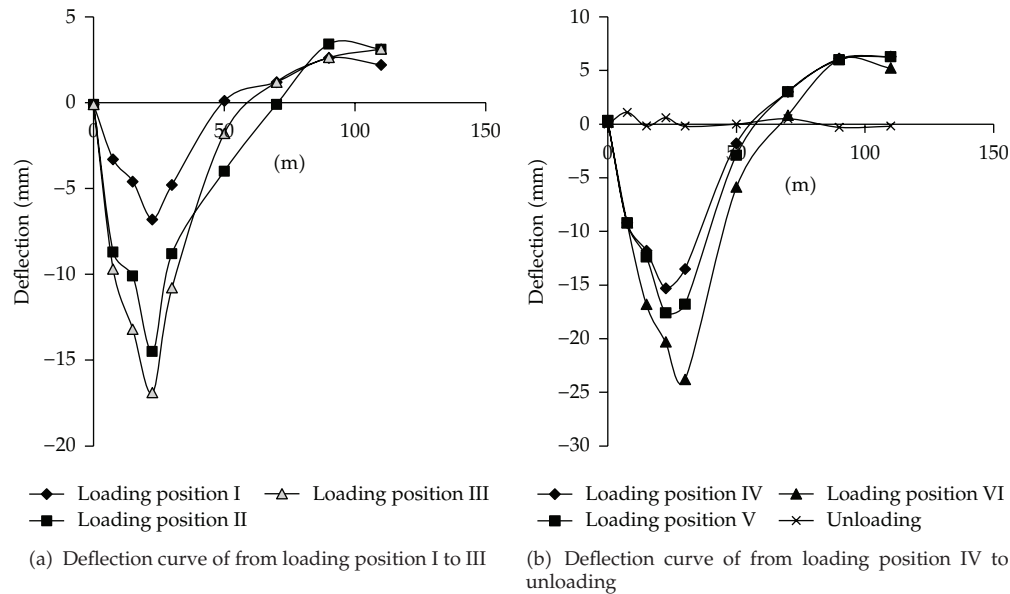
(a) Deflection curve of from loading position I to III

(b) Deflection curve of from loading position IV to unloading

Figure 10: experimental deformations under working condition I and working condition II (14-15#).

4.2. Results of Strain Test

According to the comparative analysis of the strains between the field test and theoretical analysis, the ratio β of the strain between the experimental and theoretical value is found to be within the range of the national standard (i.e., $0.7 \leq \beta \leq 1.05$). The results of measured strains show that the bridge deck strains met the requirements of design, and all strains can resume completely when the applied field loads were removed. Based on the analysis of the Quhai Bridge, the internal force (bending moment and shear force) in the deck can be obtained directly by the proposed method. Hence, the proposed method is simple and convenient. Its use can lead to a significant reduction of the analytical workload associated with solid slab bridges.

4.3. Results of Dynamic Test

Dynamic properties can be obtained by measurement of vibrations produced by ambient loads and vehicle bump. The experimental program includes dynamic characterization of the structure in normal conditions and when a half of the bridge is covered by traffic. The response of the structure was measured at 7 selected points using accelerometers. Preliminary results obtained from an FE dynamic analysis were used to determine the optimum location of the sensors. The first mode shapes of the bridge according to field dynamic test and theoretical value are presented in Table 3. The results of measured dynamic properties show that the test values of fundamental frequency for T-frame is bigger than theoretic values, but the test values of fundamental frequency for middle-span hang beam is smaller than theoretic values. This indicates that middle-span stiffness is relatively weak.
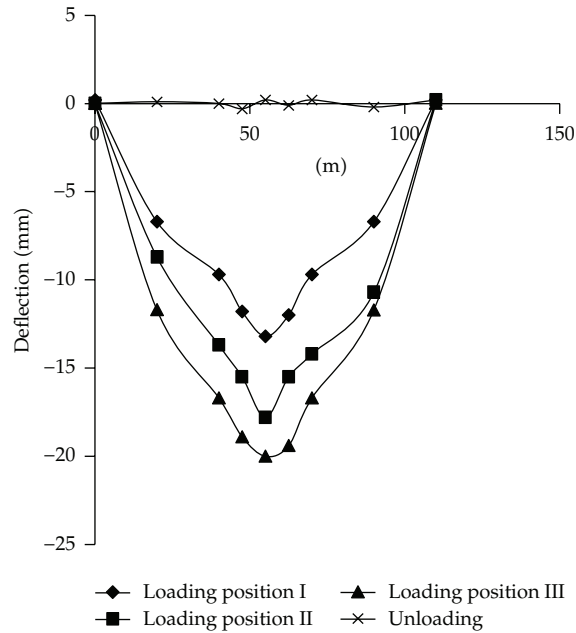
Figure 11: Experimental deformations under working condition III (15-16#).

Table 3: Experimental and theoretical base frequency (Hz).

Experiment location	Experiment	Theory	Vibration mode
15# T-frame	2.24	1.31	Symmetric vertical bending
Middle-span hang beam	2.70	3.60	Symmetric vertical bending
16# T-frame	2.22	1.30	Symmetric vertical bending

5. Conclusion

The static and dynamic behaviors of a rigid T-frame bridge were investigated analytically and experimentally. Based on the comparison study on analysis results obtained from the conventional and proposed analysis methods, one may obtain more economical designs using the spatial grillage model. Main contents of the grillage model include the grillage mesh and the grillage member section properties. The precision of the grillage model mainly lies on the simulation of the equivalent grillage stiffness and the element property. According to the comparative analysis, the bridge possesses a relatively small stiffness to resist the deformation. As a result, field test results have indicated that the bridge works in the elastic stage, but the bridge has a relatively smaller load-carrying capacity under the design load conditions. Therefore, some suggests of reinforcement or maintenance for the bridge were presented to increase bearing capacity, and prestressed outside were employed to solve deflection of beam, relatively smaller effective prestress and web shear crack. In addition, bearings of right and left hang beam were replaced to recover mechanical behavior of the original design.
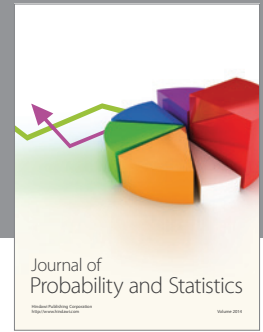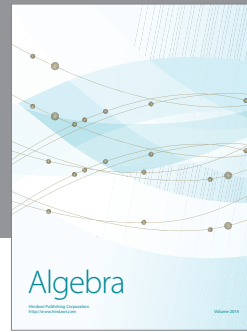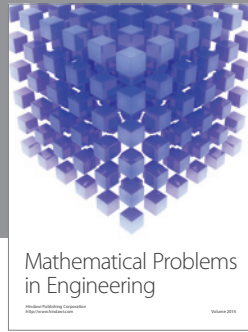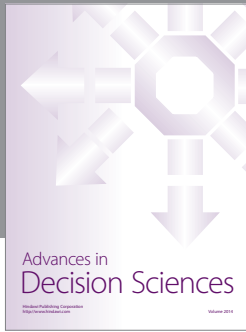
Acknowledgments

References

[1] Z. F. Pan, C. C. Fu, and Y. Jiang, "Uncertainty analysis of creep and shrinkage effects in long-span continuous rigid frame of Sutong Bridge," *Journal of Bridge Engineering*, vol. 16, no. 2, pp. 248–258, 2011.

[2] C. Cattani, S. Chen, and G. Aldashev, "Information and modeling in complexity," *Mathematical Problems in Engineering*, vol. 2012, Article ID 868413, 4 pages, 2012.

[3] S. Chen, Y. Wang, and C. Cattani, "Key issues in modeling of complex 3d structures from video sequences," *Mathematical Problems in Engineering*, vol. 2012, Article ID 856523, 17 pages, 2012.

[4] N. Azizi, M. M. Saadatpour, and M. Mahzoon, "Using spectral element method for analyzing continuous beams and bridges subjected to a moving load," *Applied Mathematical Modelling*, vol. 36, no. 8, pp. 3580–3592, 2012.

[5] T. L. Wang, D. Huang, and M. Shahawy, "Dynamic behavior of slant-legged rigid-frame highway bridge," *Journal of structural engineering*, vol. 120, no. 3, pp. 885–902, 1994.

[6] M. Dicleli, "A rational design approach for prestressed-concrete-girder integral bridges," *Engineering Structures*, vol. 22, no. 3, pp. 230–245, 2000.

[7] M. Carlini, S. Castellucci, M. Guerrieri, and T. Honorati, "Stability and control for energy production parametric dependence," *Mathematical Problems in Engineering*, vol. 2010, Article ID 842380, 21 pages, 2010.

[8] S. Y. Chen and Q. Guan, "Parametric shape representation by a deformable NURBS model for cardiac functional measurements," *IEEE Transactions on Biomedical Engineering*, vol. 58, no. 3, pp. 480–487, 2011.

[9] A. R. Cusens and R. P. Pama, *Bridge Deck Analysis*, Wiley, New York, NY, USA, 1975.

[10] M. Yoshikawa, H. Hayashi, S. Kawakita, and M. Hayashida, "Construction of Benten viaduct, rigid-frame bridge with seismic isolators at the foot of piers," *Cement and Concrete Composites*, vol. 22, no. 1, pp. 39–46, 2000.

[11] A. Kalantari and M. Amjadian, "An approximate method for dynamic analysis of skewed highway bridges with continuous rigid deck," *Engineering Structures*, vol. 32, no. 9, pp. 2850–2860, 2010.

[12] M. Mabsout, K. Tarhini, R. Jabakhanji, and E. Awwad, "Wheel load distribution in simply supported concrete slab bridges," *Journal of Bridge Engineering*, vol. 9, no. 2, pp. 147–155, 2004.

[13] AASHTO, *LRFD Design Specifications*, Washington, DC, USA, 3rd edition, 2004.

[14] C. Cattani, "Shannon wavelets for the solution of integrodifferential equations," *Mathematical Problems in Engineering*, vol. 2010, Article ID 408418, 22 pages, 2010.

[15] S. Y. Chen, J. Zhang, Q. Guan, and S. Liu, "Detection and amendment of shape distortions based on moment invariants for active shape models," *IET Image Processing*, vol. 5, no. 3, pp. 273–285, 2011.

[16] E. C. Hambly and E. Pennells, "Grillage analysis applied to cellular bridge decks," *Structural Engineer*, vol. 53, no. 7, pp. 267–274, 1975.

[17] M. P. Saka, "Theorems of structural variation for grillage systems," *Computers and Structures*, vol. 77, no. 4, pp. 413–421, 2000.

[18] L. G. Jaeger and B. Bakht, "The grillage analogy in bridge analysis," *Canadian journal of civil engineering*, vol. 9, no. 2, pp. 224–235, 1982.

[19] P. Z. Lu, J. P. Zhang, and A. R. Liu, "Structure analysis for Y-shape Bridge based on grillage theory," *Journal of Guangzhou University*, no. 2, pp. 67–72, 2006.

[20] E. Lightfoot and F. Sawko, "Structural frame analysis by electronic computer: grid frameworks resolved by generalized slope deflection," *Engineering*, pp. 18–20, 1959.

[21] E. C. Hambly, *Upper Part Bridge Structural Capability*, Communication Press, Beijing, China, 1982.